

PACS numbers: 68.08.–p; 42.62.–b; 78.20.–e; 81.07.–b
DOI: 10.1070/QE2010v040n11ABEH014444

Generation of nanostructures on metals by laser ablation in liquids: new results

E.B. Barmina, E. Stratakis, C. Fotakis, G.A. Shafeev

Abstract. **Surface nanostructuring of titanium, nickel, molybdenum, and tungsten by ablation with pico- and femtosecond laser pulses in liquids is studied experimentally for the first time. The morphology and properties of obtained nanostructures are investigated using a field emission scanning electron microscope and Raman spectroscopy. The size of nanostructures depends on the laser pulse duration and energy density and on the target material. As a rule, the size distribution of structures is bimodal. Potential applications of such nanostructured substrates are discussed.**

Keywords: *laser ablation, nanostructures, liquid.*

1. Introduction

The interaction of laser radiation with matter has been studied since the mid 60s of the last century. Among these studies are investigations of laser ablation of solids. The interaction of high-power laser radiation with matter changes the morphology of irradiated targets. As shown in [1], laser irradiation forms characteristic small- and large-scale structural elements on surfaces.

Another type of structures was observed upon laser ablation of solids in liquids by short laser pulses. Laser ablation of solids is one of the methods for synthesising nanoparticles [2]: the ablated material remains in the form of nanoparticles in the liquid surrounding the target. The generation of nanoparticles can occur under the action of laser pulses with different durations. At a pulse duration smaller than 1 ns, the formation of nanoparticles is accompanied by the appearance of self-organising nanostructures on the target surface. The average lateral size of these nanoparticles is much smaller than the laser spot diameter on the sample. Due to a small size of nanoparticles, the surface tension of the target melt can smooth them, because of which nanostructuring should be performed at small pulse durations and at energy densities close to the melting threshold of the sample material.

The nanostructuring is accompanied by a change in the target absorption spectrum (appearance of additional absorption bands near the electron plasmon resonances in nanostructures of corresponding metals) and by a change in the surface wettability. In addition, one observes enhanced Raman scattering from molecules adsorbed on nanostructured metals.

Such self-organising structures were observed for the first time on silver irradiated by 350-ps laser pulses in water [3]. In this case, the target itself became coloured and its surface remained visually smooth. The laser-irradiated regions of the target acquired a bright yellow colour. The absorption spectrum of the irradiated region showed an additional peak (at $\lambda \approx 370$ nm), which was absent in the absorption spectrum of the initial surface. The appearance of this peak testifies to the formation of nanostructures on the target surface, because its wavelength corresponds to the wavelength of plasmon oscillations of electrons in such nanostructures on silver [4].

Nanostructures were also observed on gold [5, 6] ablated with picosecond laser pulses in water. Subsequent investigations revealed enhanced Raman scattering on nanostructured silver and gold substrates with enhancement factors of 10^5 and 10^4, respectively. Later, enhanced Raman scattering with an enhancement factor of 10^8 was observed on a nanostructured nickel substrate decorated with gold [7].

Similar nanostructures were obtained on aluminium by ablation with femtosecond laser pulses in air and liquid (water, ethanol) [8, 9] and on tantalum [10].

Undeniably, nanostructured substrates are of great practical interest. For potential technological applications, nanostructures must be monodisperse and have a high generation rate, which depends on the target material. The common specific features of nanostructures formed by laser ablation of metals in liquids were studied in [3, 5–10]. However, each metal is characterised by its own physicochemical properties, which affect the process of nanostructuring.

In this work, we present new results on nanostructuring of metals upon ablation by short laser pulses in liquids.

2. Experimental technique

As targets, we used 100-μm-thick molybdenum, nickel, tungsten, and titanium plates. Prior to irradiation, their surfaces were polished. A target was placed on the bottom

E.B. Barmina, G.A. Shafeev Wave Research Centre, A.M. Prokhorov General Physics Institute, Russian Academy of Sciences, ul. Vavilova 38, 119991 Moscow, Russia; e-mail: shafeev@kapella.gpi.ru;
E. Stratakis Institute of Electronic Structure and Laser, Foundation for Research and Technology – Hellas (IESL-FORTH), P.O. Box 1527, Heraklion 711 10, Greece; Materials Science and Technology Department, University of Crete, Heraklion 710 03, Greece;
C. Fotakis Institute of Electronic Structure and Laser, Foundation for Research and Technology – Hellas (IESL-FORTH), P.O. Box 1527, Heraklion 711 10, Greece; Physics Department, University of Crete, Heraklion 714 09, Greece

Received 19 August 2010; revision received 23 September 2010
Kvantovaya Elektronika **40** (11) 1012 – 1020 (2010)
Translated by M.N. Basieva

of a glass cell, which was filled with a liquid. We used four laser radiation sources:

(i) A 1.064-μm Nd : YAG laser emitting 350-ps pulses at a pulse repetition rate of 300 Hz.

(ii) A 248-nm KrF laser emitting 5-ps pulses at a pulse repetition rate of 10 Hz.

(iii) A 800-nm Ti : sapphire laser emitting 180-fs pulses at a pulse repetition rate of 1 kHz.

(iv) The third harmonic of a 355-nm Nd : YAG laser emitting 150-ps pulses at a pulse repetition rate of 10 Hz.

In the first case, the cell was placed on a computer-controlled table to move it with a given rate perpendicular to the laser beam axis, and, in all the other cases, irradiation was performed in a stationary regime. The laser beam was focused on the target through a liquid layer several millimetres thick. The beam cross-section area on the target plane was determined from the dimensions of the modified region. The radiation of all the lasers was linearly polarised.

The surface morphology of irradiated targets was studied using a field emission scanning electron microscope (FESEM). As liquids, we used water filtered through a reverse osmosis filter and a 95 % solution of ethanol. The absorption spectra of nanostructured targets before and after irradiation by laser pulses were recorded in the region of 250 – 2500 nm on a Perkin-Elmer Lambda-950 spectrometer with an integrating sphere coated with a reference diffusion Teflon film. The reflection coefficient R was measured, and the absorption was calculated as $1 - R$. The diffuse scattering from the sample surface was taken into account. The Raman spectra of the titanium surface before and after irradiation were measured on a Nicolet Almega XR spectrometer using laser radiation with a wavelength of 473 nm.

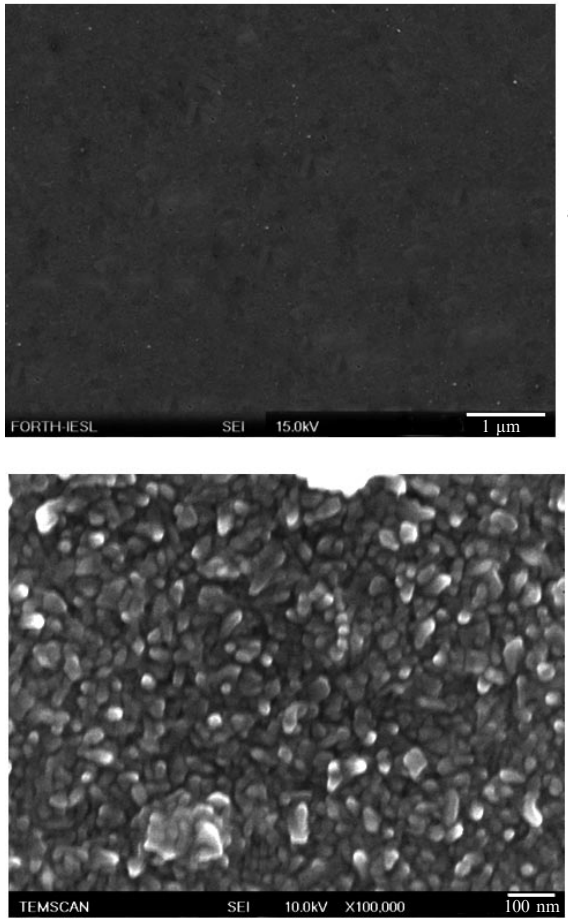

Figure 1. Nickel surface before (a) and after (b) irradiation by 350-ps pulses of a Nd : YAG laser in ethanol.

3. Results and discussion

3.1 Nanostructuring of nickel

Nickel rather actively interacts with water, because of which we mainly used ethanol as a surrounding liquid. The surface morphology of nickel before and after ablation under an ethanol layer by 350-ps pulses from a Nd : YAG laser is shown in Fig. 1.

One can see nanostructures with an average lateral size of 30 – 50 nm formed on the initially smooth nickel surface as a result of laser irradiation. It is known that the structuring character depends on the initial surface condition [3]. Therefore, we studied the effect of the initial relief on the conditions of nanostructuring on the nickel surface. For this purpose, we coated a clean surface with a photoresist, exposed it to a focused electron beam, and then developed. Next, using an electrochemical technique, we deposited nickel onto the photoresist-free regions and removed the unexposed photoresist layer. The morphology of such a substrate is shown in Fig. 2. The surface morphology after ablation by 350-ps laser pulses is shown in Fig. 3.

One can see structures with a lateral size of $\sim$150 nm formed in the grooves of the initial relief; at a particular energy density, the structuring occurred only in the region of initial seeding and did not occur on the smooth surface (see the inset in Fig. 3).

Ablation by a KrF laser with a pulse duration of 5 ps formed structures with a smaller average lateral size and a bimodal size distribution (Fig. 4). One can see that one of the distribution peaks lies near 210 nm. The structures of this size can be formed due to the interference of the laser beam with the surface electromagnetic wave (SEW) excited by the laser radiation on the target surface, since the size of these structures (210 nm) is close to the wavelength of the incident radiation (248 nm). This bimodal distribution is

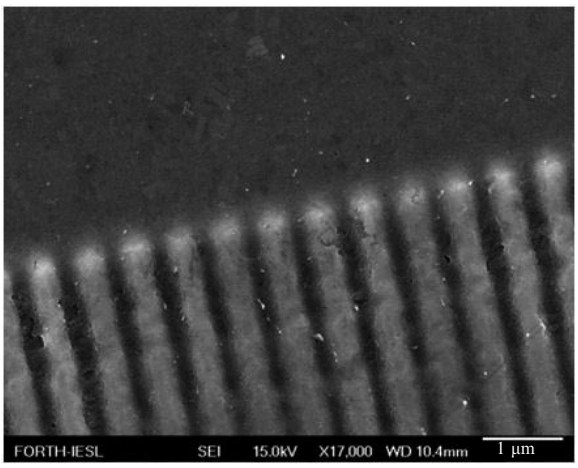

Figure 2. Nickel surface with an initial relief formed by electron-beam lithography.

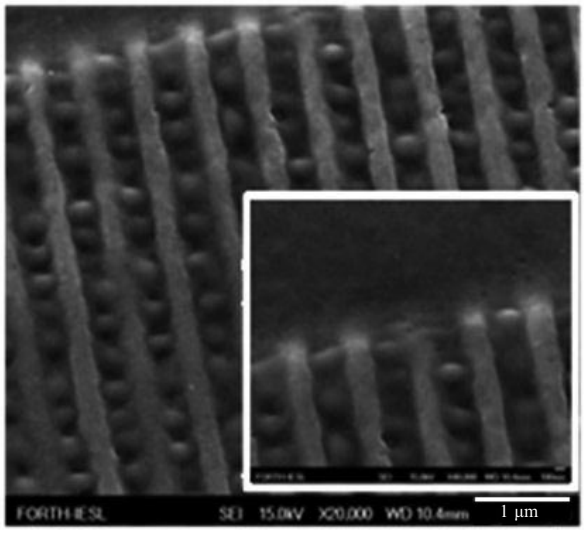

Figure 3. Nickel surface (Fig. 2) after irradiation by 350-ps Nd : YAG laser pulses in ethanol. The inset shows the boundary between the structured and initial surfaces.

typical for surface structuring under laser irradiation [11]. Figure 4 shows that each structure is surrounded by voids, whose appearance can be interpreted as a result of the pressure of the vapour of the surrounding liquid on the melt layer on the target surface. Let us estimate this pressure.

The work on the formation of a structure with a radius r is done against the melt surface tension forces. The elementary work $\mathrm{d}A$ needed to increase the length $2\pi r$ of a circular interface with a thickness $\mathrm{d}r$ can be described by the expression

$$\mathrm{d}A = \sigma 2\pi r \mathrm{d}r,$$

where σ is the coefficient of surface tension of the metal melt. The total work spent on the formation of a structure with the radius r is

$$A = 2\int_0^r \sigma 2\pi r \mathrm{d}r = 2\pi\sigma r^2, \quad (1)$$

On the other hand, this work is done by the pressure force $F = S\Delta p$, where S is the area of the nanostructure surface and Δp is the pressure difference between the relief extrema. This force acts at a distance $l = 2r$, and, hence, the work is

$$A = Fl = \pi r^2 \Delta p 2r. \quad (2)$$

From (1) and (2), we have $\Delta p = \sigma/r$. To form a nanostructure with a radius of 50 nm, the pressure difference must be equal to 80 MPa [12].

In the case of femtosecond laser irradiation, the surface morphology is somewhat different (Fig. 5). In the used energy density range, we observe no typical spherical structures. It is obviously related to a small thickness of the melt layer. It is also seen that the existence of an initial relief is really advantageous for nanostructuring, as was observed in [3] for laser nanostructuring of silver.

3.2 Nanostructuring of titanium

In the next set of experiments, we studied nanostructuring on a titanium surface upon ablation by short laser pulses.

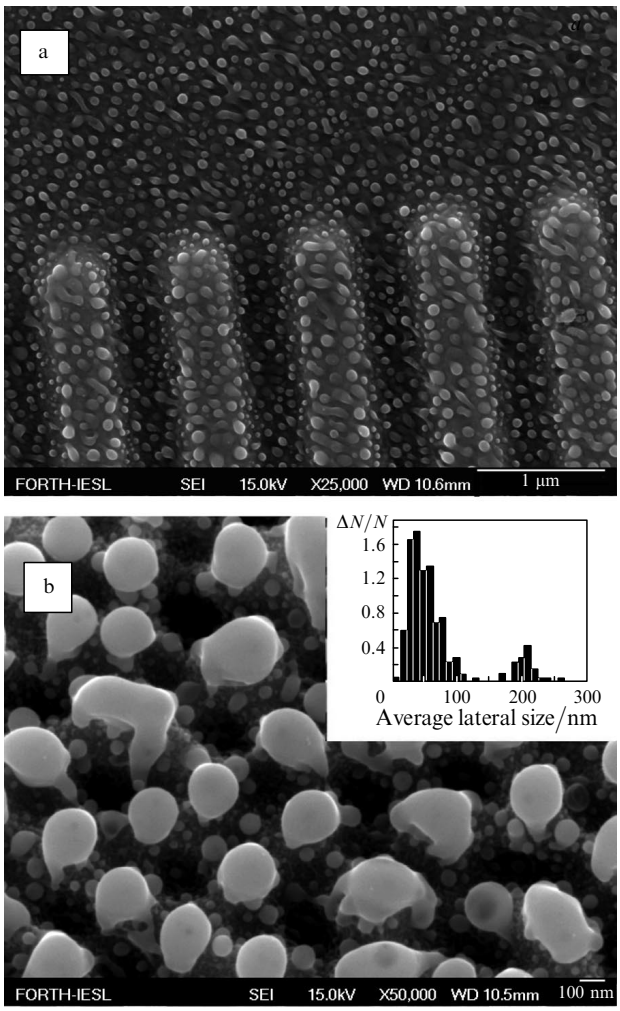

Figure 4. Front (a) and side (b) views of a nickel surface irradiated by 5-ps KrF laser pulses in ethanol. The initial surface was smooth. The inset shows the size distribution of structures ($\Delta N/N$ is the ratio of the number of structures of a particular size to the total number).

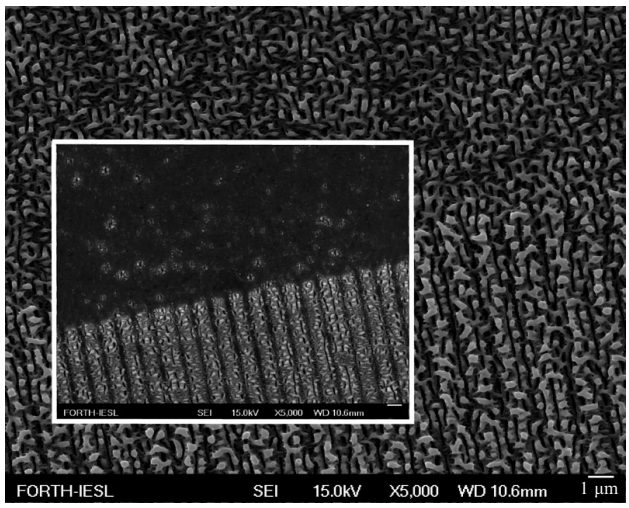

Figure 5. Nickel surface with a photolithographic initial relief after irradiation by femtosecond laser pulses in ethanol. The inset shows the nickel surface after irradiation by laser pulses with a lower energy density.

The titanium surface regions exposed to laser radiation in a liquid acquire a visible colour, whose type and intensity depend on the number of laser pulses and the chosen liquid. The coloration does not depend on the angle of the beam incidence and, hence, is not related to interference. In the case of a small number of pulses, the surface acquires a yellow colour, which, with increasing the number of pulses, changes to blue and then to violet. The absorption spectra of targets irradiated in water and ethanol are shown in Fig. 6.

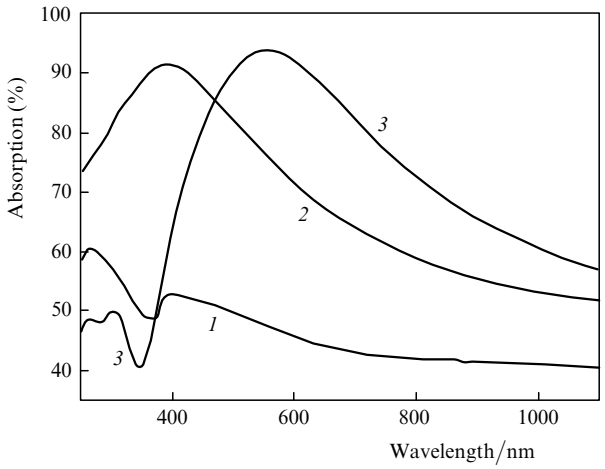

Figure 6. Absorption spectra of a titanium surface before (*1*) and after irradiation by 5-ps laser pulses in ethanol (*2*) and water (*3*).

A titanium sample that became purple after laser irradiation absorbs more than 90 % of light in the green spectral region. A similar colour was observed when a sample was irradiated by 150-ps laser pulses in water. The absorption spectrum of this surface is shown in Fig. 7. In this case, the absorption maximum lies near 530 nm, and this position corresponds to a small number of laser pulses. With increasing the number of laser pulses, the colour intensity increases and the maximum shifts to the red.

The surface morphology of titanium irradiated by picosecond laser pulses in a liquid was studied using a FESEM. Figure 8 presents the typical images of a titanium surface after irradiation in ethanol and water. As seen, the nanostructures obtained in water have a conical shape with a height of ~ 100 nm. It should be noted that the time necessary to obtain a visible colour of titanium by irradiation in ethanol is longer than in the case of irradiation in water because the laser radiation wavelength (248 nm) is close to the electronic absorption edge of the ethanol molecule.

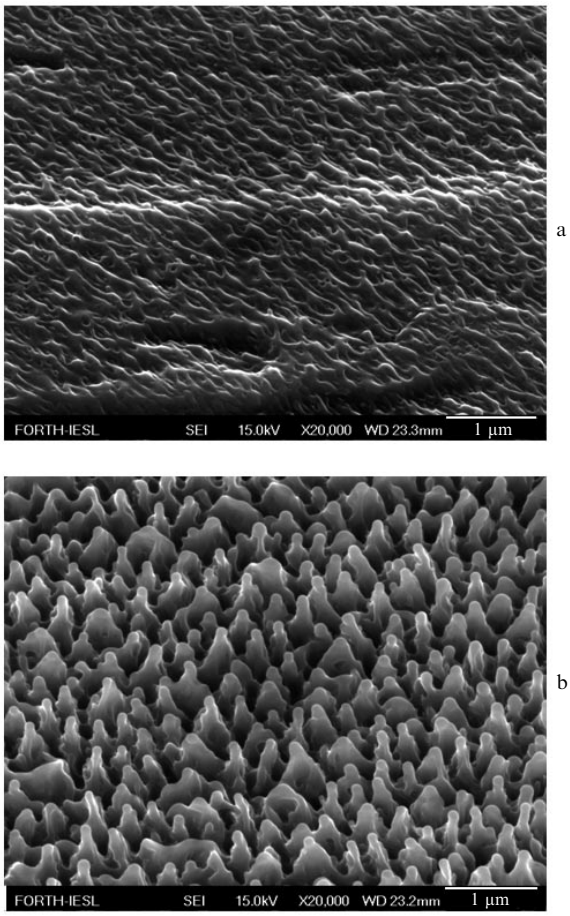

Figure 8. Surface morphology of titanium irradiated by 5-ps laser pulses in ethanol (1200 pulses, energy density 1 J cm^{-2}) (a) and water (600 pulses, energy density 0.4 J cm^{-2}) (b).

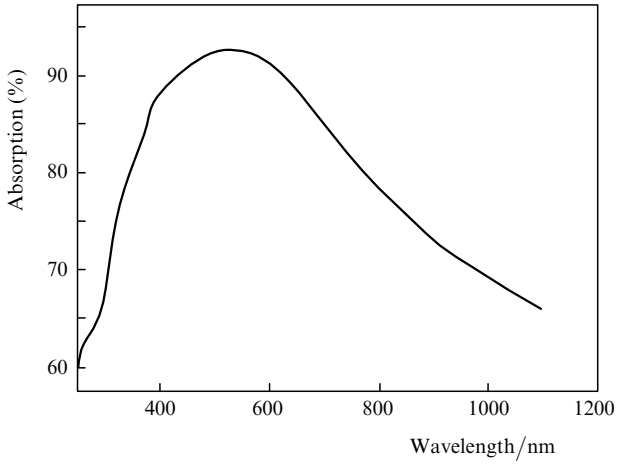

Figure 7. Absorption spectrum of a titanium surface irradiated by 150-ps, 355-nm laser pulses in water.

Figure 9 presents the titanium surfaces irradiated in water by different numbers of laser pulses with identical pulse energy densities. At a small number of pulses, the structures are vertical longitudinal plane walls of different lengths. Three-dimensional structures are formed under action of a larger number of pulses and look like a symbiosis of longitudinal plane walls with nanostructures on the top. These structures have the maximum height of 400 – 500 nm and the lateral size of ~ 100 nm. The width of these walls is also ~ 100 nm, while their length may reach 1 μm.

The dependences of the surface density of nanostructures on the number of pulses for different pulse energy densities are given in Fig. 10. One can see that even 100 pulses are enough to form a dense array of structures and that the final density of structures depends on the energy density. This dependence very rapidly reaches saturation at high energy densities and does not saturate at the lowest energy density. The saturation can occur because the high energy densities

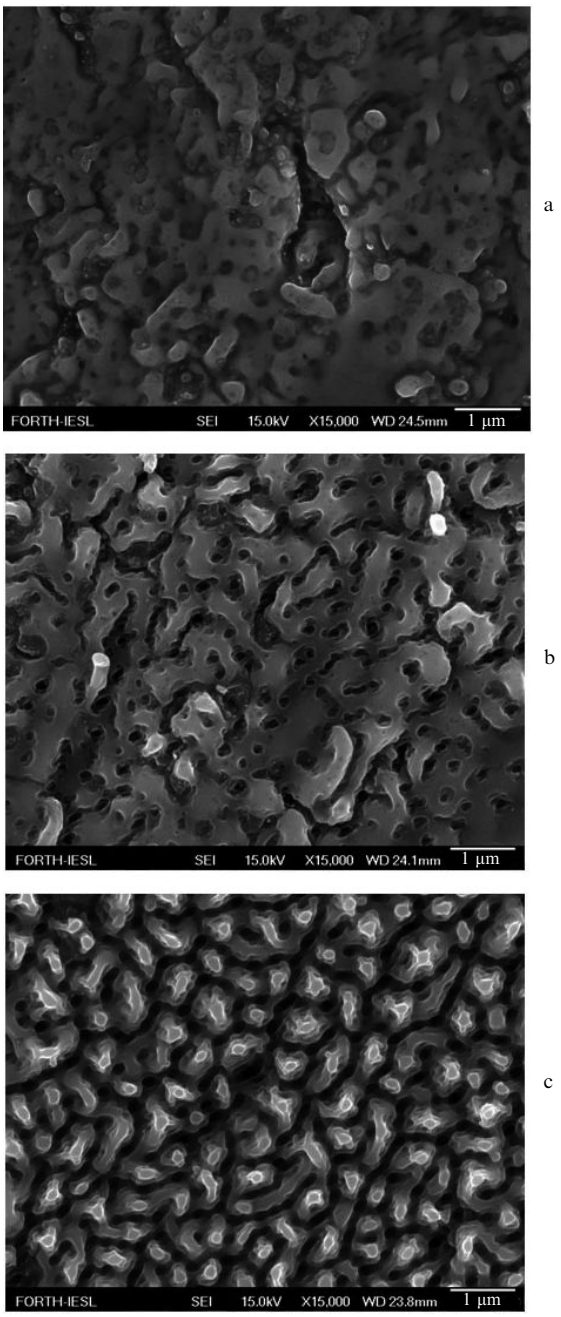

Figure 9. Evolution of structures on a titanium surface with increasing the number of laser pulses from 10 (a) to 100 (b) and 600 (c) upon ablation in water by 5-ps laser pulses with a pulse energy density of 0.15 J cm^{-2}.

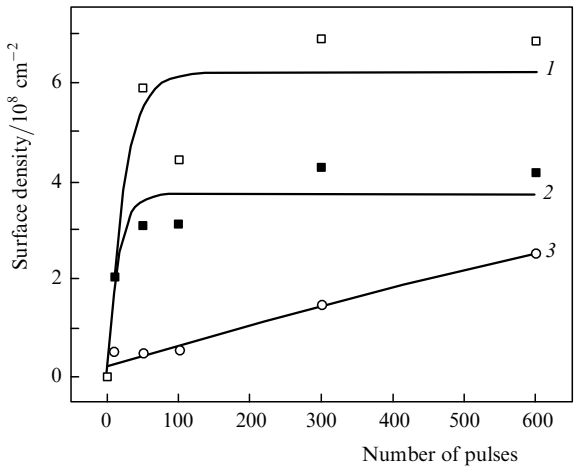

Figure 10. Surface density of nanostructures as a function of the number of 5-ps, 248-nm laser pulses with a pulse energy densities 1.32 (*1*), 0.75 (*2*), and 0.6 J cm^{-2} (*3*) upon ablation in water.

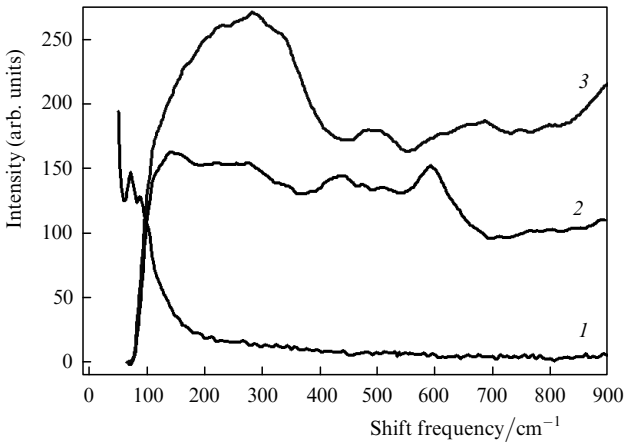

Figure 11. Raman spectra on an initial titanium surface (*1*) and on surfaces irradiated in water (*2*) and ethanol (*3*).

significantly exceed the titanium ablation threshold, because of which nanostructures in the surrounding liquid are formed with a high rate.

The nature of the coloration of samples is not completely clear. The irradiated regions can be coloured due to different reasons, for example, the coloration of nanostructured silver and aluminum [3, 8, 9] is caused by the plasmon resonance in nanostructures, but, on the other hand, in our case it can be related to the formation of oxide on the titanium surface. To determine the chemical composition of irradiated surfaces, we measured the Raman spectra of the initial and irradiated titanium surfaces of different colours. These spectra are presented in Fig. 11.

One can see that the spectrum of the initial surface has no pronounced peaks, while the spectrum of the irradiated surface is similar to the spectrum of titanium oxide (rutile TiO_2). However, the oxide layer is thin, because a thick layer would not let us observe titanium nanostructures with an FESEM due to their charging in the process of observation. In addition, rutile is transparent in the visible region and thus cannot colour the modified region.

The different absorption spectra of laser-ablated titanium regions correspond to different morphologies of nanostructures on the irradiated surfaces. Ablation in ethanol leads to yellow coloration of the sample and to the appearance of short nanowalls on its surface, while the blue colour of the target is observed in the case of longitudinal nanostructures with the length-to-width ratio 1 : 4 – 1 : 5. As is known, elongated nanoparticles are characterised by two absorption peaks, one of them corresponds to the transverse plasmon resonance and the other belongs to the longitudinal resonance. The position of the second peak depends on the ratio between the length and diameter of nanoparticles (geometric ratio): the higher this ratio, the larger the red shift of the absorption peak. This is also true for longitudinal nanostructures (nanowalls adjacent to the

target surface). One of the plasmon resonance peaks corresponds to the transverse oscillations of electrons in the wall, and the other peak corresponds to longitudinal oscillations. In particular, the absorption spectrum of a target after ablation in water (Fig. 6) includes the contribution of both longitudinal and transverse resonances in walls and nanostructures.

If the titanium colour is caused by the formation of nanostructures, then the titanium nanoparticles whose size is close to the size of the structures should have absorption bands in the visible region. The peak of the plasmon resonance of titanium spherical particles 10 nm in size lies in the UV spectral region and shifts to the visible region as the size of nanoparticles increases to 50 – 100 nm [4]. Figure 12 presents the calculated normalised absorption spectrum of spherical titanium nanoparticles 100 nm in size and the experimental absorption spectrum of the titanium surface after irradiation by laser pulses in water. The best coincidence between the positions of the calculated and experimental absorption peaks is obtained when the calculation was performed using the refractive index 1.42 for the medium surrounding the nanoparticle (this is the case shown in Fig. 12). It should be noted that the average lateral size of nanostructures on the titanium surface is ~ 100 nm (Fig. 8b). The Raman spectrum shows that the surface of nanoparticles is covered by a layer of rutile TiO_2, whose refractive index in the visible region is 2.6 rather than 1.42 expected according to the calculation. This discrepancy is obviously related to the fact that the modified surface is coated only by a thin rutile layer and its effective refractive index lies in the region of 1 – 2.6. The difference between the theoretical and experimental curves in Fig. 12 in the red region is explained by a nonideal spherical shape of nanostructures. As was mentioned above, the absorption spectrum of nanostructured titanium has two different plasmon peaks, which are responsible for the transverse resonance and for the longitudinal oscillations of electrons. The longitudinal plasmon peak should be shifted to the red with respect to the transverse peak, which well agrees with the experimental data presented in Fig. 12.

It is very likely that the irradiation of a titanium target by 300-ns laser pulses [13] forms on the target surface nanostructures involved in the coloration of the modified region. Titanium easily evaporates in the case of laser heating at an energy density of 300 J cm^{-2}, which was used in [13], and the recoil vapour pressure can be responsible for nanostructuring. The spatial resolution of images presented in [13] does not allow one to make a conclusion on the presence of such structures. It should be noted that, in the case of 300-ns laser pulses, the formed oxide layer is thick enough to observe its well pronounced X-ray diffraction peaks. On the other hand, the action of picosecond laser pulses on a titanium surface in a liquid leads to the formation of a thinner oxide layer. This is caused both by a smaller partial pressure of oxygen in the liquid (which does not exceed the limit of oxygen solubility in water) and by a smaller lifetime of the melt. Therefore, the colour of the modified region must be caused by the formation of nanostructures rather than by the existence of an oxide layer or by the interference in it.

It is interesting to note that the coloration of a titanium surface corresponding to Fig. 12 can also be observed under completely different experimental conditions, for example, under irradiation of a titanium target in vacuum by femtosecond laser pulses with a rather high energy density. The surface morphology of such a target before and after irradiation is shown in Fig. 13. As seen, the initial surface is smooth and does not contain any inclusions or particles. Under laser irradiation, the titanium target material evap-

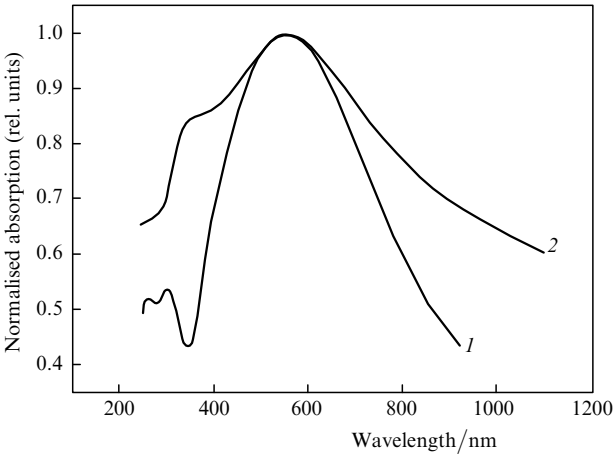

Figure 12. Calculated normalised absorption spectrum of titanium nanoparticles 100 nm in diameter (*1*) and experimental absorption spectrum of a nanostructured titanium substrate irradiated in water by 5-ps laser pulses (*2*).

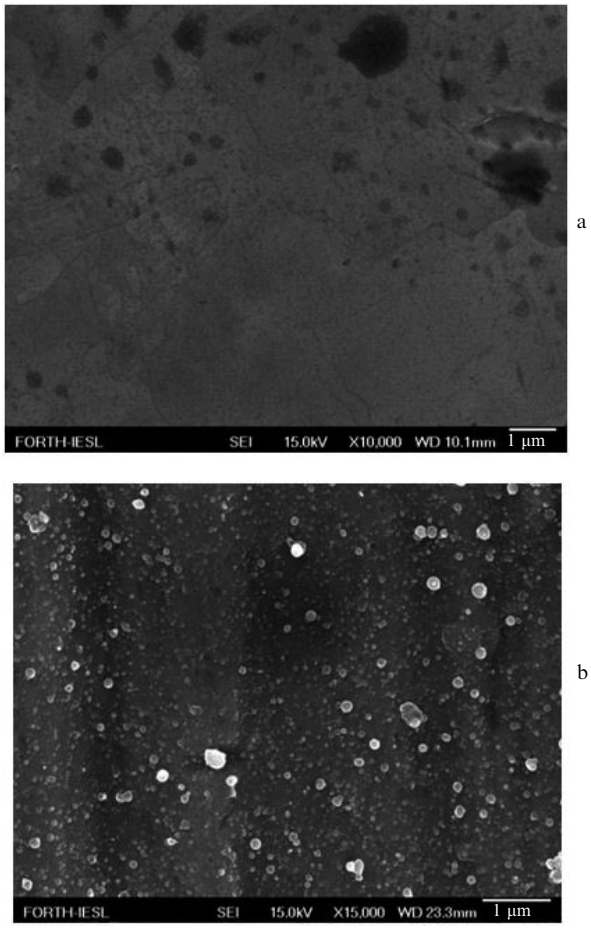

Figure 13. Surface morphology of a titanium target before (a) and after irradiation in vacuum by femtosecond laser pulses (b). In Fig. 13b, one can see ablated target material deposited on the unirradiated region.

orates and the ablated particles (nanoclusters 30 – 50 nm in diameter) cover the target surface around the irradiated region (Fig. 13b). In this region, one observes all the colours acquired by titanium substrates upon ablation by picoseconds pulses in liquids, from yellow far from the irradiated region to dark-violet near this region. The absorption spectrum of this substrate is given in Fig. 14.

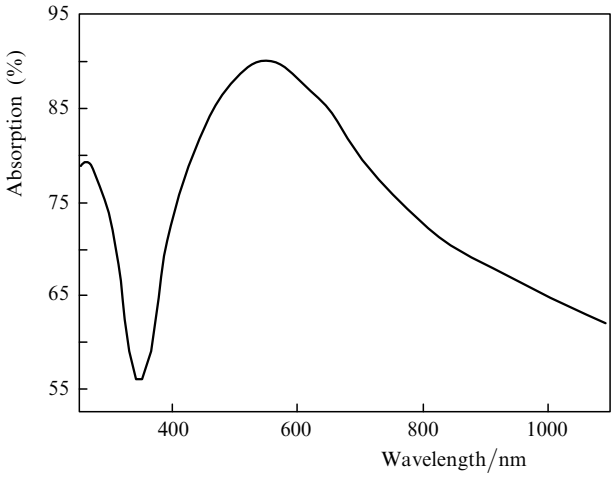

Figure 14. Absorption spectrum of a titanium surface irradiated by femtosecond laser pulses.

One can see that the absorption spectrum of the titanium surface covered by clusters is similar to the spectra observed after ablation of titanium in water, and the position of the spectral peak points to the average size of titanium clusters on the substrate surface. Thus, the presence of nanoclusters makes a contribution to the substrate coloration, and the colour depends on the size of these clusters.

The region of the titanium target irradiated in vacuum by femtosecond laser pulses becomes black. This is caused by the formation of microcones on the surface. The surface morphology is shown in Fig. 15. It is covered by periodic microcones, whose surfaces are modulated by small-scale periodic structures. Such microstructures were also previously observed on titanium surfaces irradiated by nanosecond laser pulses [14].

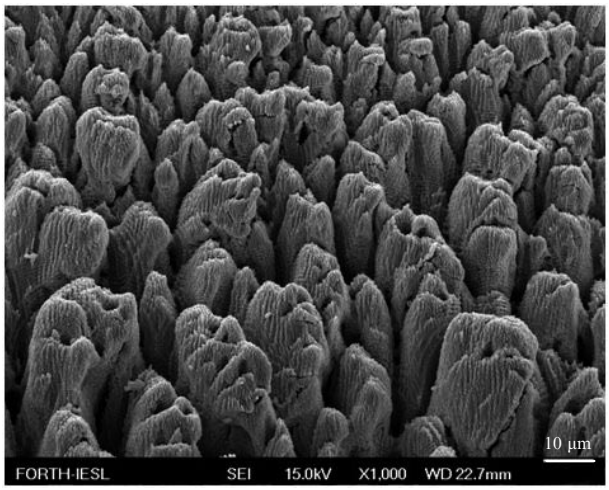

Figure 15. Titanium surface after ablation by femtosecond laser pulses in vacuum.

The Raman spectrum of titanium ablated by femtosecond laser pulses in vacuum is similar to the Raman spectra of titanium laser-irradiated in water. Figure 16 shows the Raman spectra for two regions with different visible colours (red and blue). The common peaks at 140 and 620 cm^{-1} correspond to the Raman peaks of rutile. The clusters hardly oxidise during laser irradiation in vacuum, they obviously oxidise after removing the target from the vacuum chamber. In this case, the oxide layer thickness does not exceed the natural thickness of oxide on titanium and is equal to several nanometers.

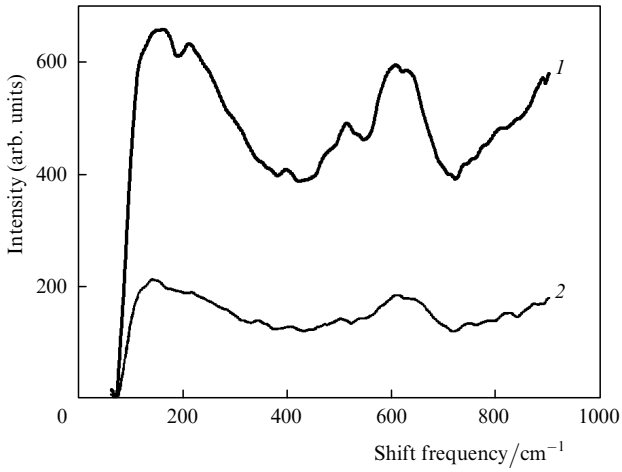

Figure 16. Raman spectra of the blue (*1*) and red (*2*) titanium ablated by femtosecond laser pulses in vacuum.

Figure 16 shows that the Raman spectra recorded on the titanium surface decorated with nanostructures belong to oxides of different compositions. The total thickness of the oxide layer should be close to the thickness of the natural oxide on the initial titanium surface, since the target undergoes the action of short laser pulses at a high temperature and the oxidation occurs for a short time. As was mentioned above, a thick oxide layer would not let one observe titanium nanostructures using a FESEM because they charge during observation. Note also that the initial surface shows no Raman peaks (Fig. 11). The high intensity of oxide peaks in the Raman spectra (compared to the intensity of the Raman peak for the initial titanium surface, which is also oxidised) can be explained by a field enhancement near nanostructures lying under the titanium oxide layer. Thus, the intense Raman peaks of oxides are observed because, first, the area of the nanostructured titanium surface is larger than the area of the initial surface and, second, the Raman signal can be enhanced on the nanostructures of metal titanium. In this case, the titanium oxide Raman signal is enhanced if oxide lies in the immediate vicinity of metal nanostructures.

3.3 Nanostructuring of molybdenum

Figure 17 demonstrates the surface morphology of molybdenum irradiated by 5-ps laser pulses in water. The nanostructures look like quasi-periodic nanospheres with an average size of ~ 200 nm. The surface density of structures is 3×10^{12} cm^{-2}, which is noticeably higher

than the density of nanostructures on other metals (except for gold and silver). By electrodeposition of nickel on a nanostructured molybdenum surface, one can obtain a ferromagnetic substrate with a dense pattern of structures. If one nanostructure carries one bit of information, the recording density is 1 Tbit cm^{-2}, which considerably exceeds the recording density of existing devices.

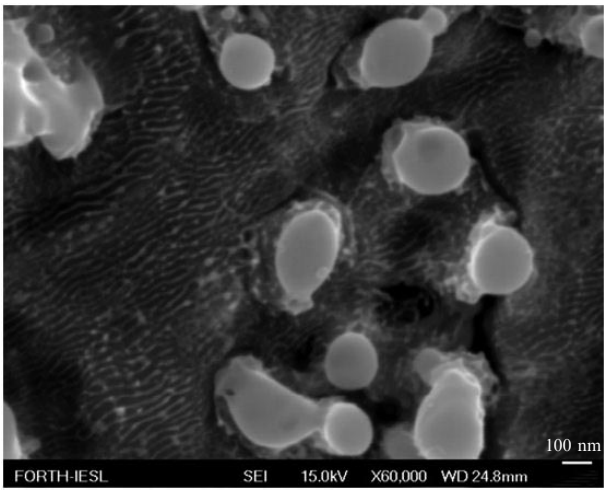

Figure 17. Molybdenum surface after irradiation by 5-ps, 248-nm laser pulses in water.

The size distribution of molybdenum nanostructures is shown in Fig. 18. In this case, there is only one peak near 210 nm. Note that structures with a size of the order of the incident laser radiation wavelength are absent. Probably, this relates to a high SEW decay coefficient in this metal. As a rule, the interference between a laser wave and a SEW leads to the appearance of the second peak in the size distribution function of structures. The morphology of nanostructures on the molybdenum surface differs from the morphology of nanostructures observed on other metals. In Fig. 17, attention should be paid to the formation of small-scale bands with a period of 25 nm.

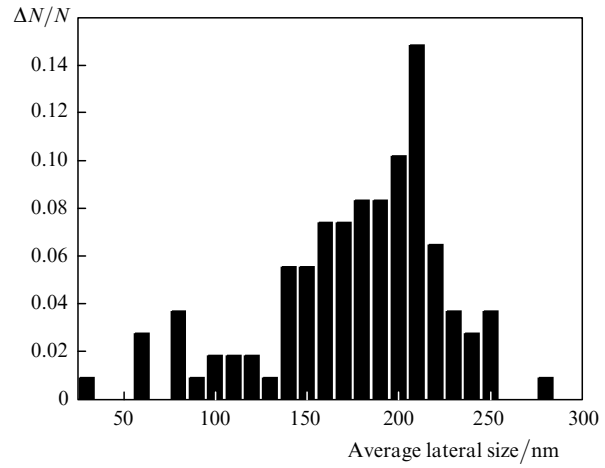

Figure 18. Normalised size distribution of structures over a molybdenum surface irradiated in water by 5-ps laser pulses.

3.4 Nanostructuring of tungsten

Interest to nanostructuring of tungsten is related to its wide application as an electron emitter, in particular, a field emitter. The formation on nanohillocks leads to a local enhancement of the electric field around them, which will allow one to improve the characteristics of industrial cathodes.

Figure 19 presents the surface morphology of tungsten immersed in water and irradiated by 180-fs laser pulses at a wavelength of 800 nm. The tungsten surface morphology is typical for metals irradiated by femtosecond laser pulses [10]. Instead of a dense array of sphere-like structures, one observes only small-scale periodic structures, which can be formed by the interference of the laser wave with the SEW excited by the laser radiation on the target surface. The period of these structures is ~ 350 nm. In Fig. 19b, in the grooves between the longitudinal structures, one can distinguish periodic (with a period of ~ 25 nm) structures perpendicular to the grooves.

The absorption spectrum of the modified tungsten region is shown in Fig. 20. As seen, nanostructuring leads to a shift of the absorption maximum from the UV region to longer wavelengths, which is reflected in the appearance of a yellow colour of the sample [3, 8, 9] and in a 30 % increase in its absorbing ability.

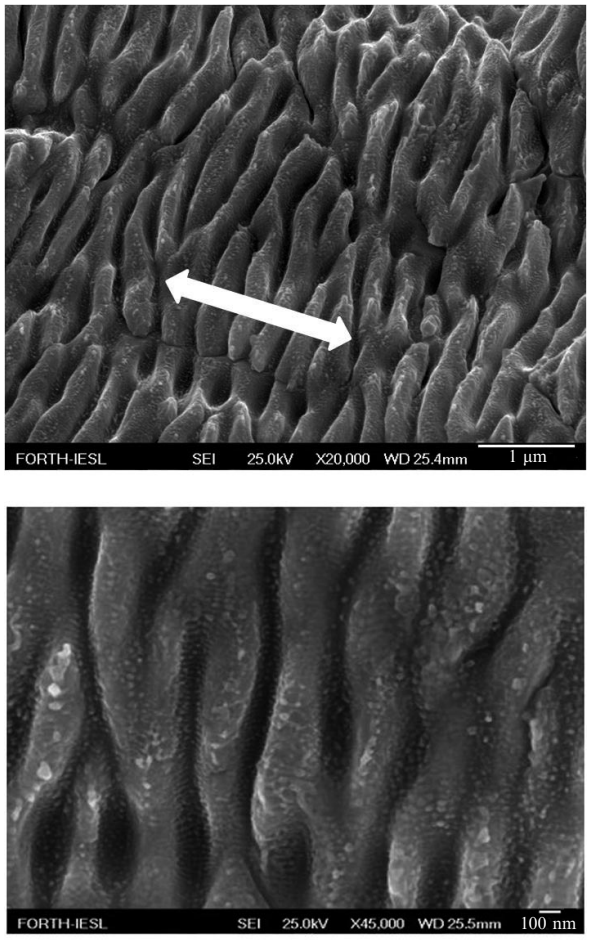

Figure 19. Tungsten surface after irradiation in water by femtosecond laser pulses (a) and a region of this surface on an enlarged scale (b). The arrow shows the direction of the laser radiation polarisation.

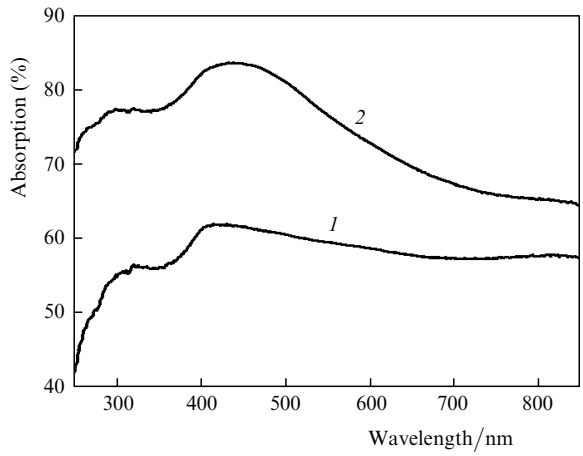

Figure 20. Absorption spectra of an initial tungsten surface (*1*) and of a surface region irradiated in water by 180-fs laser pulses (*2*).

4. Conclusions

Thus, we experimentally studied nanostructures on titanium, tungsten, molybdenum, and nickel formed by ablation with pico- and femtosecond laser pulses in liquids. The average lateral size of the structures is 50 – 200 nm depending on the substrate material. The morphology and density of the structures depend on the number and duration of laser pulses, as well as on the radiation energy density on the target. It is found that, in the case of titanium irradiated in liquids, the colour of the modified region appears due to plasmon oscillations of electrons in nanostructures. The high density of structures allows one to use such substrates as magnetic data recording media and as field electron emitters.

Acknowledgements. The authors thank A.V. Simakin, P.G. Kuz'min, and M. Barberoglou for their help in the experiments and useful discussions. This work was partly supported by the Russian Foundation for Basic Research (Grant No. 10-02-90044).

References

1. Akhmanov S.A., Emel'yanov V.I., Koroteev N.I., Seminogov V.N. *Usp. Fiz. Nauk*, **147**, 675 (1985) [*Sov. Phys. Uspekhi*, **28** (12), 1084 (1985)].
2. Shafeev G.A., in *Encyclopedia of Nanotechnology* (New York, 2010) pp 991 – 1026.
3. Zavedeev E.V., Petrovskaya A.V., Simakin A.V., Shafeev G.A. *Kvantovaya Elektron.*, **36** (10), 978 (2006) [*Quantum Electron.*, **36** (10), 978 (2006)].
4. Creighton A., Eadon D.G. *J. Chem. Soc. Faraday Trans.*, **87**, 3881 (1991) .
5. Truong S.Lau, Levi G., Bozon-Verduraz F., Petrovskaya A.V., Simakin A.V., Shafeev G.A. *Appl. Phys. A*, **89** (2), 373 (2007).
6. Truong S.Lau, Levi G., Bozon-Verduraz F., Petrovskaya A.V., Simakin A.V., Shafeev G.A. *Appl. Surf. Sci.*, **254**, 1236 (2007).
7. Barmina E.V., Truong C. Lau, Bozon-Verduraz F., Levi G., Simakin A.V., Shafeev G.A. *Kvantovaya Elektron.*, **40** (4), 346 (2010) [*Quantum Electron.*, **40** (4), 346 (2010)].
8. Stratakis E., Zorba V., Barberoglou M., Fotakis C., Shafeev G.A. *Appl. Surf. Sci.*, **255**, 5346 (2009).
9. Stratakis E., Zorba V., Barberoglou M., Fotakis C., Shafeev G.A. *Nanotechnology*, **20**, 105303 (2009).
10. Barmina E.V., Barberoglou M., Zorba V., Simakin A.V., Stratakis E., Fotakis C., Shafeev G.A. *Kvantovaya Elektron.*, **39** (1), 89 (2009) [*Quantum Electron.*, **39** (1), 89 (2009)].
11. Emel'yanov V.I., in *Phase Transitions Induced by Short Laser Pulses* (New York: Novapublishers Inc., 2009) pp 181 – 226.
12. Barmina E.V., Barberoglou M., Zorba V., Simakin A.V., Stratakis E., Fotakis C., Shafeev G.A. *J. Optoelectron. Adv. Mater.*, **12** (3), 496 (2010).
13. Del Pino P., Serra R., Morenza J.L. *Appl. Surf. Sci.*, **197-198**, 887 (2002).
14. Voronov V.V., Dolgaev S.I., Lavrischev S.V., Lyalin A.A., Simakin A.V., Shafeev G.A. *Appl. Phys. A*, **73**, 177 (2001).